DOI:10.1002/ejic.201201350

Synthesis, Characterization, and Catalytic Behavior of Dioxomolybdenum Complexes Bearing AcAc-Type Ligands

Ties J. Korstanje,[a] Emma Folkertsma,[a] Martin Lutz,[b] Johann T. B. H. Jastrzebski,[a] and Robertus J. M. Klein Gebbink*[a]

Keywords: Sustainable chemistry / Dehydration / Alcohols / Molybdenum / Alkenes / O ligands

A series of $[MoO_2(acac')_2]$ [acac′ = acetylacetonato-type ligand: dibenzoylmethane (**3**), 1-benzoylacetone (**4**), bis(*p*-methoxybenzoyl)methane (**5**), 2-acetylcyclopentanone (**6**), 2-acetylcyclohexanone (**7**), and 2-acetyl-1-tetralone (**8**)] complexes have been synthesized in yields of 44–83 % by a simple synthetic method by using sodium molybdate and the desired acac-type ligand as starting materials. All the complexes were characterized by IR, UV/Vis, NMR, and high-resolution ESI-MS, and for compounds **3**, **4**, and **8**, solid-state structures were obtained by X-ray diffraction. All the complexes contain a *cis*-dioxomolybdenum moiety, as proven by the characteristic Mo=O vibrations in the IR spectra and the occurrence of four sets of signals in the NMR spectra of the complexes bearing asymmetrical ligands (**4** and **6**–**8**), and confirmed by the solid-state structures. The complexes were found to be active as catalysts in the dehydration of 1-phenylethanol to styrene using technical-grade toluene as the solvent in air at 100 °C. The highest catalytic activity was found for $[MoO_2\{(t\text{Bu}CO)_2CH\}_2]$ (**2**), followed by $[MoO_2\{(C_6H_5\text{-}CO)_2CH\}_2]$ (**3**). Both complexes were also found to be active in the dehydration of other alcohols, including allylic, aliphatic, and homoallylic alcohols, as well as secondary and tertiary alcohols, with **2** generally showing better activity and selectivity than **3**. These catalytic results were compared with those previously obtained with the metal-based catalyst Re_2O_7 and the benchmark acid catalyst H_2SO_4. The results were dependent on the substrate: By using **2**, good selectivities but lower activities were generally obtained with tertiary alcohols, whereas good activities but lower selectivities were obtained with secondary alcohols. The industrially important dehydration of 2-octanol to octenes was very efficiently catalyzed by **2**. Overall, the $[MoO_2(acac')_2]$ complexes reported herein could offer a cheaper and more abundant metal-based catalyst alternative to the previously reported rhenium-based catalytic system for the dehydration reaction.

Introduction

As a result of the increasing scarcity of fossil resources, currently the main provider of building blocks for the chemical industry, considerable research effort is being focused on the use of biomass as an alternative source of chemical building blocks. Lignocellulosic biomass, in particular, could provide sufficient sustainable carbon-based material on an annual basis.[1,2] The major challenge in the substitution of fossil resources by lignocellulosic biomass lies in the structural differences between the two: Fossil resources contain mostly underfunctionalized, oxygen-poor scaffolds, whereas lignocellulosic biomass is highly functionalized and oxygen-rich in the form of hydroxy groups. For lignocellulosic biomass to be a convenient resource for the chemical industry, part of the functionality needs to be removed or converted and its oxygen content needs to be lowered. One of the methods for accomplishing this is by dehydration of the hydroxy groups to yield olefinic moieties (Scheme 1).

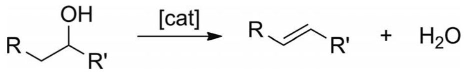

Scheme 1. Dehydration of alcohols to olefins.

Commonly, the dehydration reaction is performed with strong (solid) acid catalysts, such as mineral acids,[3] zeolites,[4] or metal oxides.[5,6] The major drawback of these methods is their low selectivity and low functional group tolerance as well as their acidic nature, which causes reactor corrosion and safety concerns. More selective catalysts for the dehydration of alcohols under mild conditions are therefore desirable.

Few transition-metal-catalyzed dehydration reactions have been reported; and those that have are based on the use of zinc,[7] ruthenium,[8] or rhenium.[9–13] We have previously reported on the use of rhenium-based catalysts in

---

[a] Organic Chemistry & Catalysis, Debye Institute for Nanomaterials Science, Utrecht University,
Universiteitsweg 99, 3584 CG Utrecht, The Netherlands
Fax: +31-30-2523615
E-mail: r.j.m.kleingebbink@uu.nl
Homepage: http://www.uu.nl/science/occ
[b] Crystal and Structural Chemistry, Bijvoet Center for Biomolecular Research, Utrecht University,
Padualaan 8, 3584 CH Utrecht, The Netherlands

Supporting information for this article is available on the WWW under http://dx.doi.org/10.1002/ejic.201201350.

the dehydration reaction; we found high-valence rhenium catalysts to be highly active as well as selective in the dehydration of various alcohols.[14,15] Comparison with traditional (solid) acid catalysts such as sulfuric acid, acid resins, and zeolites showed that rhenium(VII) oxide, the most active rhenium-based catalyst, is more active and more selective than any of the acidic catalysts tested. However, the limited natural abundance of rhenium could restrict the use of rhenium-based catalysts. Molybdenum, like rhenium, is located in the middle of the transition-metal block of the Periodic Table and as such is active in oxygen atom transfer (OAT) reactions such as oxidation and deoxygenation. In addition, [MoO_2(acac)$_2$] has been reported as a catalyst for the dehydration of tertiary alcohols.[16] In nature, molybdenum-containing enzymes, usually bound by the pterin cofactor, are known to be active in OAT reactions, for example, in dmso reductase and sulfite oxidase.[17] In this paper we report on our investigations into the use of molybdenum-based catalysts for the dehydration of alcohols to olefins.

Results and Discussion

Catalysis – Commercially Available Complexes

Initially, our investigation of molybdenum-based catalysts was focused on the dehydration of 1-phenylethanol to styrene using commercially available molybdenum complexes (Table 1). Screening for solvent, temperature, and the presence or absence of air with [MoO_2(acac)$_2$] (**1**) as catalyst revealed the following optimal reaction conditions: Technical-grade toluene as the solvent, 100 °C as the reaction temperature, and an ambient atmosphere (1 atm. air), which is similar to the optimal conditions found earlier by us for the rhenium-based catalysts.[14]

By using these conditions, we tested various commercially available molybdenum materials in the dehydration reaction. Molybdenum metal (Table 1, entry 1) showed little activity in the dehydration of 1-phenylethanol, as did sodium molybdate (entry 2). Surprisingly, molybdenum(VI) oxide also showed little activity (entry 3), although rhenium(VII) oxide had performed very well in this reaction. Molybdenum(VI) dichloride dioxide, in contrast, showed good activity, giving almost complete conversion after 24 h and a high initial rate of 5.43 mmol h^{-1} but with a poor selectivity for styrene (entry 4), and accordingly a poor mass balance. This is likely caused by oligo- or polymerization of the styrene formed under the given reaction conditions. [MoO_2(acac)$_2$] (**1**) and [MoO_2\{(tBuCO)$_2$CH\}$_2$] (**2**), both [MoO_2(acac′)$_2$] complexes, showed similar activity, but somewhat improved selectivity for styrene (entries 5 and 6). In comparison with sulfuric acid (entry 7), the two molybdenum complexes bearing acac-type ligands show higher activity with a 2.5-fold lower catalyst loading, although the styrene selectivity was somewhat higher with sulfuric acid. The trend in activity of the tested compounds appears to follow the previously observed trend in rhenium-catalyzed dehydration, which is linked to the Lewis acidity of the catalyst.[15] Molybdenum metal is a poor Lewis acid, as is the anionic molybdate salt, and both show low activity. The high-valence molybdenum complexes are stronger Lewis acids and show good activity. The only complex that falls out of this trend is molybdenum(VI) oxide, which is a strong Lewis acid, but shows low activity.

Synthesis and Characterization of the [MoO_2(acac′)$_2$] Complexes

Because the two [MoO_2(acac′)$_2$] complexes **1** and **2** were the best performing catalysts tested in our initial dehydration tests, we decided to adapt the acac-type ligand to optimize the catalytic behavior of these complexes.

A simple synthetic method adapted from previously reported methods[18,19] using sodium molybdate as the metal precursor and the acetylacetonate preligand in stoichiometric amounts in an acidic water/ethanol mixture yielded two previously reported (**3** and **4**)[19] and four novel (**5–8**) [MoO_2(acac′)$_2$] complexes in moderate-to-good yields (Figure 1). An alternative method involving halide abstraction from MoO_2Cl_2 with the help of Ag(OTf)$_2$ and subsequent

Table 1. Dehydration of 1-phenylethanol to styrene catalyzed by commercially available molybdenum complexes.[a]

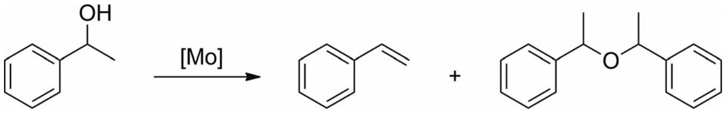

Entry	Catalyst	Catalyst loading [mol-%]	Time [h]	Conversion[b] [%]	Styrene selectivity[b] [%]	Turnover number[b] (TON)	Initial rate[b,c] [mmol h^{-1}]
1	Mo^0	5	22	23	35	5	<0.1
2	Na_2MoO_4	5	22	12	8	2	<0.1
3	MoO_3	5	22	32	10	6	<0.1
4	MoO_2Cl_2	1	24	96	21	96	5.43
5	[MoO_2(acac)$_2$] (**1**)	1	24	97	30	97	5.16
6	[MoO_2\{(tBuCO)$_2$CH\}$_2$] (**2**)	1	22	>99	28	99	6.77
7	H_2SO_4	2.5	24	>99	39	25	3.65

[a] Reaction conditions: 2 mmol 1-phenylethanol, 0.02–0.1 mmol catalyst, 250 µL pentadecane (as internal standard), 10 mL toluene, 100 °C. [b] Based on GC. [c] Rate of consumption of starting material during the first 5 min of reaction.

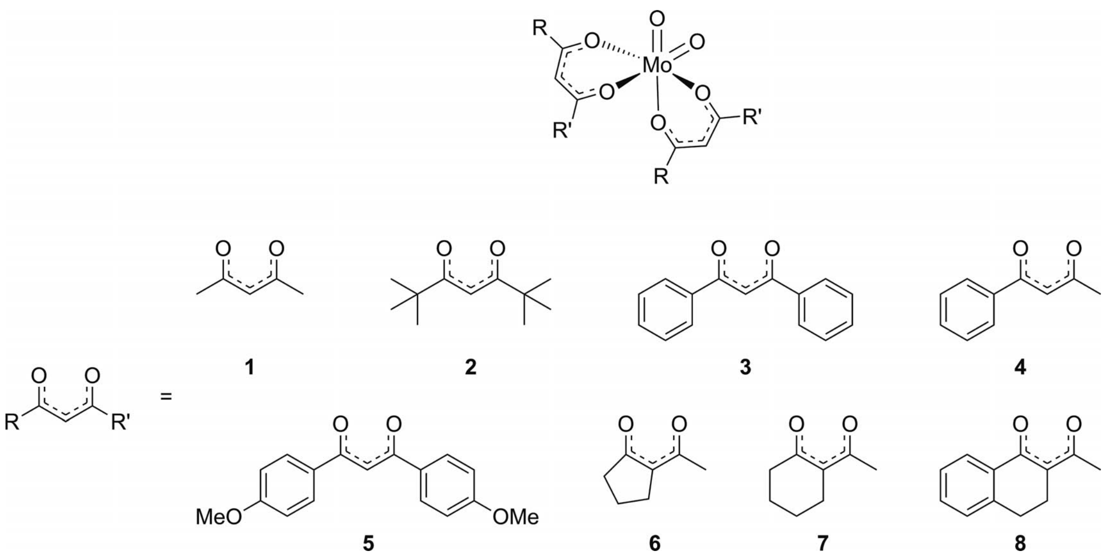

Figure 1. [$MoO_2(acac')_2$] complexes **1**–**8**.

addition of the desired ligand did not yield the desired compounds.

All the isolated complexes show a very strong doublet in the IR spectrum in the 895–940 cm^{-1} region (Table 2), which can be attributed to the symmetrical and anti-symmetrical vibrations of the MoO_2 moiety. The observed frequency range is indicative of the *cis* conformation of the MoO_2 moiety; the *trans* conformation would be lower in energy (790–820 cm^{-1}) due to less overlap of the lone pairs of the oxo ligand with the d orbitals of the metal, which reduces the π donation of the oxo ligands and thus lowers the Mo=O bond order.[20] The *cis* conformation is most common for dioxo d^0 metal complexes of this type.[19] Considerable differences in the Mo=O vibrational energies of the complexes are observed, ranging from 893 to 907 cm^{-1} for the anti-symmetrical Mo=O vibration and from 927 to 940 cm^{-1} for the symmetrical Mo=O vibration. The anti-symmetrical and symmetrical Mo=O vibrations in these complexes are correlated, with the exception of complex **7**, which has the lowest anti-symmetrical but the highest symmetrical Mo=O vibration energy. The IR spectra of the four complexes bearing an aromatic moiety in the ligand backbone (**3**–**5** and **8**) show similar characteristics with an anti-symmetrical Mo=O vibration at around 898 cm^{-1} and a symmetrical vibration at around 927 cm^{-1}. The very small difference between the Mo=O vibrational energies of **3** and **5** is surprising as the *p*-methoxy groups on the phenyl rings of **5** have a strong electron-donating effect, which is expected to influence the electron density on the metal center and therefore the Mo=O bond energy. The similarity between these two complexes indicates that the π systems of the phenyl rings do not influence the binding to the metal, likely because it is not delocalized onto the enolate π system.

Table 2. IR and UV/Vis data of the [$MoO_2(acac')_2$] complexes, sorted by the symmetrical Mo=O vibration.

	Infrared		UV/Vis
	antisym Mo=O [cm^{-1}]	sym Mo=O [cm^{-1}]	λ_{max} [nm] (ε [$L\,cm^{-1}\,mol^{-1}$])
7	893	940	289 (1.65×10^3), 778 (329)
2	907	936	322 (6.71×10^3)
6	901	935	332 (4.38×10^5), 777 (264)
1	902	932	322 (6.84×10^3)
3	898	929	376 (2.97×10^4), 346 (2.01×10^4)
4	899	927	346 (4.73×10^4)
5	899	927	380 (4.08×10^4), 363 (4.73×10^4)
8	897	927	376 (1.47×10^4)

Considerable differences in the maximum absorption energies are observed in the UV/Vis spectra of the complexes, varying from 289 nm for compound **7** to 380 nm for compound **5**. These transitions can be attributed to π–π* transitions in the enolate ligands. Furthermore, the colors of the isolated complexes are different, ranging from yellow (**2**) to dark blue (**6**). The two complexes bearing cycloalkyl derivatives (**6** and **7**) both show an additional absorption at 777 and 778 nm, respectively. This absorption can be attributed to the presence of small amounts of polyoxomolybdates, also known as molybdenum blue, which are known to have strong absorptions in this region due to an intervalence charge-transfer (IVCT) transition.[21] Therefore it is likely that the inherent colors of **6** and **7** are not blue and green, respectively, but yellow, similar to the color of the other complexes. We also observed the rapid decomposition of complexes **6** and **7** by NMR spectroscopy (see below), which explains the occurrence of these species and thus their apparent color.

When comparing the trends in the symmetrical Mo=O vibrations and the UV/Vis absorption maxima, it can be observed that the Mo=O vibration energy increases with increasing UV/Vis absorption maximum. This trend can be rationalized as follows: A low-energy absorption corresponds to a small energy difference between the π and π* orbitals of the ligand as a result of an elevated orbital energy of the HOMO in the case of an electron-rich system.

Likewise, an electron-rich ligand system would donate more electron density to the empty d orbitals of the metal center, thereby lowering the π donation of the lone pairs of the oxo ligands to the d orbitals of the metal, thereby resulting in a lower bond order and thus a lower vibrational energy.

In the case of the complexes bearing unsymmetrical ligands, that is, **4** and **6**–**8**, three different geometrical isomers incorporating a *cis*-MoO_2 moiety can be formed, each of which has an enantiomer (Figure 2). This is illustrated by the NMR spectra of these compounds, which contain four sets of signals (one set for OC6–22 and OC6–33 each, and another two sets for OC6–23[22] due to the nonequivalence of the ligands in this conformation). The complexes bearing symmetrical ligands (**3** and **5**) have only one geometrical isomer, as illustrated by a single signal for the central CH proton. For the aryl protons of **3** and **5**, a double set of signals is observed due to the nonequivalence of the two aryl rings in the dibenzoylmethane ligands. During the NMR measurements, some decomposition of the complexes was observed, hampering the acquisition of ^{13}C NMR spectra. Various solvents were tested to minimize the decomposition during the measurement, with dry, oxygen-free [D$_8$]thf proving to be the optimal solvent. However, as a result of the moderate solubility of the complexes in organic solvents, combined with the good solubility of the free ligand, ^{13}C NMR spectroscopic data were only successfully obtained for complexes **3** and **4**. For complexes **5**–**7**,

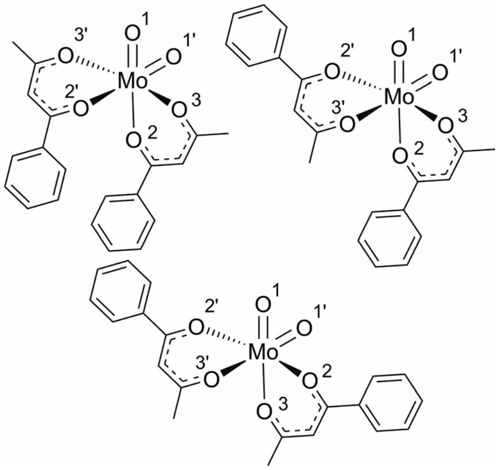

Figure 2. Three different diastereoisomers of **4**: OC6–22, OC6–23, and OC6–33 (only the Δ enantiomers are shown).[22]

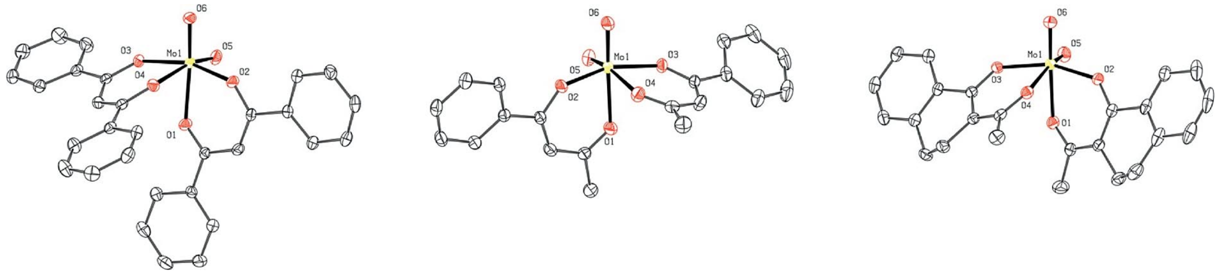

Figure 3. X-ray crystal structures of **3** (left), **4** (middle), and **8** (right). Ellipsoids are drawn at the 50% probability level. Hydrogen atoms have been omitted for clarity.

Table 3. Details of the crystal structure data collection for **3**, **4**, and **8**.

	3	**4**	**8**
Formula	$C_{30}H_{22}MoO_6$	$C_{20}H_{18}MoO_6$	$C_{24}H_{22}MoO_6$
M_r	574.42	450.28	502.36
Crystal color	yellow	yellow	yellow
Crystal size [mm^3]	0.33 × 0.33 × 0.24	0.30 × 0.09 × 0.06	0.16 × 0.13 × 0.03
T [K]	110(2)	150(2)	150(2)
Crystal system	monoclinic	monoclinic	monoclinic
Space group	$P2_1/c$ (no. 14)	$P2_1/c$ (no. 14)	Cc (no. 9)
a [Å]	9.31711(8)	9.8489(3)	10.6197(8)
b [Å]	13.26512(16)	12.4838(3)	27.201(2)
c [Å]	20.2515(8)	16.3720(4)	7.6064(6)
β [°]	96.358(1)	116.188(1)	113.841(2)
V [Å^3]	2487.54(10)	1806.34(9)	2009.8(3)
Z	4	4	4
$D_{calcd.}$ [g cm^{-3}]	1.534	1.656	1.660
$(\sin\theta/\lambda_{max})$ [Å^{-1}]	0.65	0.65	0.65
Reflections measured/unique	71874/5708	37210/4154	18504/4149
Parameters/restraints	334/0	246/0	283/2
R_1/wR_2 [$I > 2\sigma(I)$]	0.0209/0.0541	0.0271/0.0590	0.0194/0.0472
R_1/wR_2 [all reflections]	0.0271/0.0582	0.0419/0.0654	0.0207/0.0477
Flack x[27]	–	–	0.15(2)
S	1.066	1.023	1.081
ρ(min/max) [e Å^{-3}]	–0.30/0.57	–0.49/0.59	–0.24/0.37

significant amounts of protonated ligand were also observed in their ^{1}H NMR spectra. Together with the occurrence of the protonated ligand, we also observed a more symmetrical molybdenum species, likely due to a [MoO_2(acac′)] species. As a result of the observed sensitivity towards decomposition for some of the complexes, analytically pure compounds were difficult to obtain, although we succeeded in obtaining X-ray crystal structures for three of the complexes.

We determined the solid-state structures of compounds **3**, **4**, and **8** by X-ray crystal structure analysis (Figure 3). A summary of the crystallographic data are given in Table 3 and selected bond lengths and angles are given in Table 4. In all cases a distorted octahedral coordination around the molybdenum is observed, which is in accordance with the previously determined solid-state structures of similar compounds, including **1**,[23,24] **2**,[25] and **3**.[26] Although the crystal structure of **3** was reported earlier, the structure presented here is of much higher quality. In the measured crystals, only one isomer was found, OC6–33 for both **4** and **8**. The solid-state structures confirmed that all the complexes contain a *cis*-MoO_2 moiety, as was shown by IR spectroscopy. The Mo1–O5 and Mo1–O6 bond lengths [1.6984(16)–1.7057(12) Å] show the presence of a double bond and thus confirm the presence of the oxo groups. The two oxygen atoms of the acac-type ligand are not equivalent, as shown by the significant differences in the Mo–O bond lengths, with the longer Mo–O bond *trans* to the oxo ligand. This is most likely caused by the strong *trans* influence of the oxo ligands, which weakens and thus lengthens the C–O bond *trans* to the oxo ligands.

Table 4. Selected bond lengths and angles for **3**, **4**, and **8**.

Bond lengths [Å]	3	4	8
Mo1–O1	2.1661(11)	2.2049(16)	2.1905(16)
Mo1–O2	1.9847(11)	1.9847(15)	1.9873(15)
Mo1–O3	1.9981(10)	2.0052(14)	2.0094(15)
Mo1–O4	2.1496(11)	2.1653(16)	2.1463(16)
Mo1–O5	1.7057(12)	1.6984(16)	1.7025(16)
Mo1–O6	1.6991(11)	1.7012(16)	1.7036(16)
Bond angles [°]			
O1–Mo1–O2	81.06(4)	81.35(6)	78.82(6)
O2–Mo1–O6	93.38(5)	94.08(7)	93.31(7)
O6–Mo1–O3	99.17(5)	98.44(7)	99.91(7)
O3–Mo1–O1	83.13(4)	83.46(6)	85.03(6)
O1–Mo1–O5	89.14(5)	86.83(7)	87.20(7)
O5–Mo1–O6	104.69(6)	104.06(8)	103.90(8)
O6–Mo1–O4	91.17(5)	92.17(7)	93.97(7)
O4–Mo1–O1	75.25(4)	77.22(6)	75.67(6)
O1–Mo1–O6	165.72(5)	168.82(7)	167.54(7)
O4–Mo1–O5	163.85(5)	163.04(7)	161.24(7)

Catalysis with [MoO_2(acac′)$_2$]

After successfully synthesizing complexes **3**–**8**, they were tested as catalysts in the dehydration reaction of 1-phenylethanol to styrene (Table 5).

Table 5. Dehydration of 1-phenylethanol to styrene catalyzed by [MoO_2(acac′)$_2$].[a]

Complex	Time [h]	Conversion [%]/TON[b]	Styrene selectivity [%][b]	Initial rate [mmol h^{-1}][b,c]
3	24	98	30	5.43
4	24	99	29	3.89
5	24	>99	34	0.73
6	20	98	35	2.32
7	20	>99	30	3.77
8	24	98	30	1.21

[a] Reaction conditions: 2 mmol 1-phenylethanol, 0.02 mmol catalyst, 250 µL pentadecane (used as internal standard), 10 mL toluene, 100 °C. [b] Based on GC. [c] Rate of consumption of starting material during the first 5 min of reaction.

All six complexes showed significant catalytic activity in the dehydration of 1-phenylethanol to styrene, reaching nearly complete conversion within 20–24 h, similar to the results described above for **1** and **2**. The observed selectivity for styrene was also very similar, that is, between 29 and 35%, with complexes **5** and **6** being the most selective. In terms of activity, a larger difference is observed: Complex **3** showed an initial rate of 5.43 mmol h^{-1}, which is similar to **1**, whereas **5** showed an almost eight-fold lower activity. Complexes **4** and **7** showed somewhat lower activity than **3**, but still higher than the benchmark catalyst sulfuric acid. On the basis of these results, it was decided to use the two most active catalysts (**2** and **3**) to explore the substrate scope in the dehydration reaction.

A wide variety of alcohols, ranging from allylic, aliphatic, and homoallylic alcohols as well as secondary and tertiary alcohols, were tested in the dehydration reaction with **2** or **3** as the catalyst (Table 6). The tertiary allylic and aliphatic alcohols and both the secondary and tertiary allylic alcohol reacted readily at 100 °C, with both catalysts showing quite similar catalytic performance. In the case of the tertiary allylic alcohol 1-vinylcyclohexanol, good results were obtained with full conversion and a good selectivity for the desired olefin after 24 h with **2** as catalyst and a moderate selectivity with **3** as catalyst (entry 1). The tertiary aliphatic alcohol 3-ethylpentan-3-ol, however, showed a much lower conversion and initial rate with both catalysts, but again a good selectivity for 3-ethylpent-2-ene with **2** as catalyst and a moderate selectivity with **3** as catalyst (entry 2). In the case of the secondary allylic alcohol 1-octen-3-ol, no dehydration products were observed. Instead a 1,3-transposition to 2-octen-1-ol was observed (entry 3). After 15–60 min, selectivities of 90 and 79% were obtained with 22 and 25% conversion with **2** and **3**, respectively, as catalyst. When the reaction time was increased, the conversion was higher, but the selectivity lower. The cyclic secondary allylic alcohol 2-cyclohexen-1-ol, however, did undergo dehydration to 1,3-cyclohexadiene with high conversion and activity with both catalysts but with low selectivity (entry 4). In all cases, no other products were observed by GC, which indicates the formation of higher-boiling products resulting from oligomerization of the olefins.

Table 6. Dehydration of allylic, aliphatic, and homoallylic alcohols catalyzed by **2** or **3**.[a]

Entry	Substrate	Major product	Cat.	T (°C)	Time	Conv. (%) / TON[b]	Sel. (%)[b]	Initial rate (mmol h^{-1}) [b,c]
1	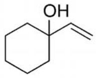	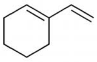	**2** **3**	100	24 h	>99 >99	73 53	5.99 5.20
2	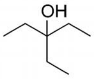	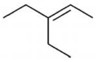	**2** **3**	100	24 h	32[d] 12[d]	75[d] 49[d]	<0.01 0.18
3	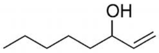	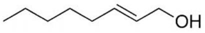	**2** **3**	100	15' 60'	22 25	90 79	1.48 0.42
4	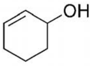		**2** **3**	100	45'	90 94	19 17	11.2 11.1
5	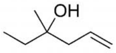	–	**2** **3**	150 100	24 h	78 6	–	n.d.[e]
6	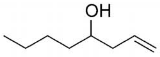	octadienes	**2** **3**	150	24 h	24 24	10[f] 14[f]	n.d.[e]
7	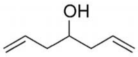	heptatrienes	**2** **3**	150	24 h	19 25	>99[f] 94[f]	n.d.[e]
8	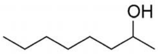	1-octene *cis*-2-octene *trans*-2-octene *trans*-3-octene	**2** **3**	150	24 h	88 14	21 / 21 31 / 24 36 / 42 6 / 28[g]	n.d.[e]

[a] Reaction conditions: 2 mmol substrate, 0.02 mmol **2** or **3**, 250 µL pentadecane (used as internal standard), 10 mL toluene, 100–150 °C, 24 h, all values averaged over two runs. [b] Based on GC. [c] Rate of consumption of starting material during the first 5 min of reaction. [d] Determined by NMR spectroscopy using 1,3,5-trimethoxybenzene as internal standard. [e] Not determined. [f] Mixture of isomers, quantified after hydrogenation using 10 wt.-% Pd on activated carbon. [g] For catalyst **3**: mixture of 3- and 4-octenes were obtained.

An interesting substrate was 3-methyl-5-hexen-3-ol (entry 5). This tertiary homoallylic alcohol did not show any reaction at 100 °C with **2**, but with **3**, some conversion was obtained. With **2**, the reaction did proceed at 150 °C with good conversion, but in both cases the reaction products could not be identified by GC.

The secondary aliphatic alcohols did not show any reaction at 100 °C with either catalyst, but upon increasing the temperature to 150 °C and by carrying out the reaction in an autoclave, these alcohols did convert. The secondary homoallylic alcohols 1-octen-4-ol and 1,6-heptadien-4-ol gave olefinic products, although the conversions were low with both catalysts after 24 h (entries 6 and 7). In the first case, a low selectivity for octadienes (10–14%) was obtained with both catalysts, but in the latter case good selectivities of 94–99% for heptatrienes were observed. In the case of the secondary aliphatic alcohol 2-octanol, poor conversion was obtained with **3** as catalyst, but very good results were obtained with **2** as catalyst, achieving 88% conversion after 24 h and in total 92% selectivity for octenes (entry 8). As 2-octanol can be obtained from castor oil,[28] this dehydration process could be industrially interesting for the production of bio-based 1-octene, which is used as a co-polymer for the production of linear low-density polyethylene (LLDPE).[29]

A comparison between **2** and **3** as catalysts in the dehydration of these alcohols shows that **2** is the superior catalyst, especially at the higher temperatures required for the secondary alcohols to react. An explanation for this difference can be found in the stability of the complexes, with **3** decomposing more rapidly at 150 °C than **2**, thus giving lower conversions.

By comparing the results obtained here with **2** and **3** (1 mol-%) as catalysts with those previously obtained with both Re_2O_7 (0.5 mol-%) and H_2SO_4 (2.5 mol-%),[15] some differences in reactivity can be observed. For tertiary alcohol substrates (entries 1 and 2), a lower activity (using the initial rate as the measure) is observed in the molybdenum-catalyzed dehydration reactions, whereas with secondary alcohols (entries 3 and 4), higher rates than with H_2SO_4, yet lower than with Re_2O_7 are observed. Notwithstanding the higher activities observed for the molybdenum catalyst compared with H_2SO_4, the conversions are much lower. Remarkably, the tertiary homoallylic alcohol 3-methyl-5-hexen-3-ol (entry 5) does not react with the molybdenum catalyst until 150 °C, whereas with both Re_2O_7 and H_2SO_4, the reaction is observed at 100 °C. For secondary homoallylic alcohol substrates (entries 6 and 7), conversions are again lower with the molybdenum catalyst, but in the case of 2-octanol (entry 8), the conversion after 24 h is comparable to that of Re_2O_7 and H_2SO_4.

In terms of product selectivity, significant differences are also observed. For the tertiary allylic alcohol 1-vinylcyclohexanol (entry 1) and the secondary allylic alcohol 1-octen-3-ol, the selectivities with the molybdenum catalyst are in between those obtained with Re_2O_7 and H_2SO_4, whereas with the aliphatic tertiary alcohol 3-ethyl-3-pentanol (entry 2) and the secondary allylic alcohol 2-cyclohexen-1-ol (entry 4), the selectivities are lower. On the other hand, for secondary homoallylic alcohols (entries 6 and 7), mixed results were obtained: For 1-octen-4-ol, the selectivity is much lower, whereas the dehydration of 1,6-heptadien-4-ol results in excellent selectivity, and much higher than with Re_2O_7 or H_2SO_4. In the industrially most interesting case, 2-octanol, the molybdenum catalyst shows good results in terms of selectivity, matching that of Re_2O_7 and surpassing H_2SO_4.

Following these observations, an explanation for the poor activity observed with tertiary alcohols might be found in steric factors, as tertiary alcohols are sterically quite hindered and the molybdenum catalysts are also quite demanding in a steric sense due to the presence of four *tert*-butyl (**2**) or phenyl (**3**) groups. This could hamper substrate approach and binding and, accordingly, the overall catalytic activity. Furthermore, the good initial rates in combination with the moderate conversions with some substrates suggest the decomposition of the catalyst under the reaction conditions. It is known that **1** can thermally decompose.[30] One of the proposed structures of this decomposition product is a $[Mo^V{}_2O_3(acac)_4]$ species, based on EPR measurements. In these measurements, a free radical, possibly an acetylacetone radical, is also observed.[31] Another proposed decomposition pathway could involve a photochemical reaction,[32] yielding a $[Mo^VO_2(acac')]$ species, also by a radical pathway. Finally, any type of polyoxomolybdate could be formed by oxidation under the reaction conditions as these are known to give an intense blue color.[21] During the dehydration reactions we observed that all tested $[MoO_2(acac')_2]$ complexes change color, in the case of **1** from yellow to green, and in the case of **2** from green to dark blue, which indicates the transformation or decomposition of the complexes. This might be the cause for the moderate conversions in some cases, although good conversions were obtained in other cases.

Based on the observations described herein we have proposed a catalytic cycle for the dehydration reaction (Scheme 2). As the molybdenum starting complex $[MoO_2(acac')_2]$ is coordinatively saturated, one of the acac-type ligands has to be expelled to allow for coordination of the alcohol. In this ligand exchange, the alcohol hydroxy proton is transferred to the acac-type ligand, which is expelled as acetylacetone. This step could provide an explanation for the high activities of **2** and **3**, as these complexes carry the most bulky ligands, which facilitates the ligand-exchange step. Next, the olefin product is expelled from the molybdenum center with the formation of a hydroxymolybdenum species. From this species, two possible pathways can occur. One is the direct coordination of another alcohol molecule to reproduce the alkoxymolybdenum intermediate following removal of water. The other possibility is coordination of acetylacetone to reproduce the original $[MoO_2(acac')_2]$ complex, which also involves the expulsion of water. In any of these ligand-exchange steps, the catalyst could be prone to decomposition due to oxidation, dimerization, or oligomerization, as described above, thereby reducing the overall catalytic activity.

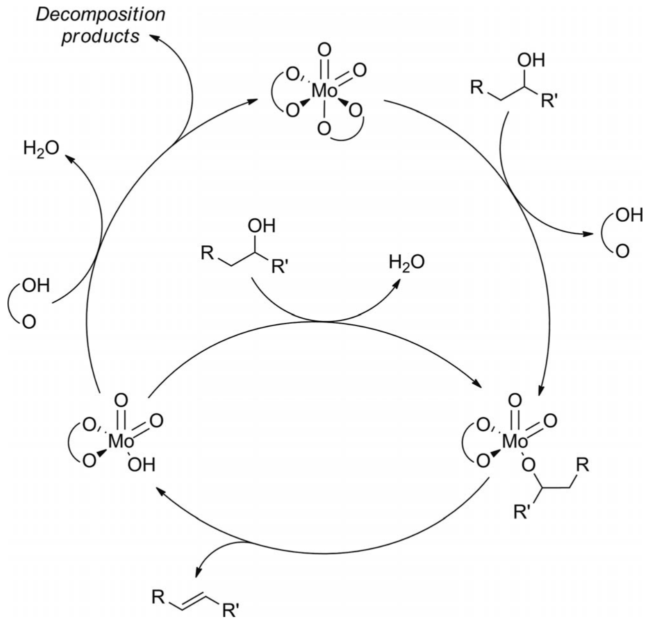

Scheme 2. Proposed catalytic cycle for the $[MoO_2(acac')_2]$-catalyzed alcohol-to-olefin dehydration reaction.

Conclusions

We have reported herein the synthesis of a series of $[MoO_2(acac')_2]$ complexes and their characterization by using various spectroscopic techniques (IR, UV/Vis, NMR), high-resolution ESI-MS, and, for complexes **3**, **4**, and **8**, X-ray diffraction. These complexes were used in the dehydration of 1-phenylethanol to styrene alongside a number of commercially available molybdenum materials and were found to be active in this reaction. The most active catalysts tested in this study were $[MoO_2\{(tBuCO)_2CH\}_2]$ (**2**) and $[MoO_2\{(C_6H_5CO)_2CH\}_2]$ (**3**), which accordingly were tested in the dehydration of a series of alcohol substrates, varying from allylic to aliphatic and homoallylic as well as both secondary and tertiary alcohols. The catalytic performances of both catalysts were compared on the basis of activity and selectivity with the results obtained previously with Re_2O_7 or H_2SO_4 as catalyst[15] and were found to give moderate results with some substrates, whereas with other substrates, such as the dehydration of 2-octanol to octenes using **2**, comparable results to Re_2O_7 were obtained. Amongst other dehydrative transformations, this opens up the possibility of using a cheaper and more abundant metal, such as molybdenum, for the industrially important dehydration of 2-octanol to octenes without sacrificing selectivity.

Experimental Section

General: Bis(*p*-methoxybenzoyl)methane was prepared by a literature procedure.[33] All other starting materials were obtained from commercial sources and used without further purification. Dry diethyl ether and thf were obtained from an MBraun MB SPS-800 solvent purification system, $[D_8]$thf was dried by distillation from sodium/benzophenone and stored over 4 Å molecular sieves. ^1H and ^{13}C NMR spectra were recorded at 298 K with a Varian AS 400 MHz NMR spectrometer at 400 and 100 MHz, respectively. Chemical shifts are reported in ppm and referenced against the residual solvent signal. IR spectra were recorded with a Perkin–Elmer Spectrum One FT-IR spectrometer operated in ATR mode. UV/Vis spectra were recorded with a Varian Cary50 Scan UV/Vis spectrometer. GC analysis was performed with a Perkin–Elmer Autosystem XL Gas Chromatograph equipped with an Elite-17 column (30 m × 0.25 mm × 0.250 µm) and a flame ionization detector. GC–MS analysis was performed on a Perkin–Elmer Autosystem XL Gas Chromatograph equipped with an AT-50 column (30m × 0.25 mm × 0.25 µm) and a Perkin–Elmer TurboMass Upgrade. ESI mass spectra were recorded in acetonitrile with a Waters LCT Premier XE KE317 Micromass Technologies spectrometer. Owing to the poor stability of these complexes in solution, as described in the Results and Discussion section, no suitable elemental analysis data was obtained.

General Synthetic Procedure: A modified literature method was used for the synthesis of complexes **3**–**8**.[19] A solution of dibenzoylmethane (3.38 g, 15.1 mmol) in absolute ethanol (60 mL) was added during 5 min to a colorless solution of sodium molybdate dihydrate (1.09 g, 7.65 mmol) in 0.5 M HCl (45 mL, 22.6 mmol). A yellow precipitate was formed and the suspension was cooled to –30 °C overnight. The yellow solution was decanted and the bright-yellow solid was dried in a vacuum desiccator over phosphorus pentoxide overnight. The dried solid was washed three times with diethyl ether until the filtrate remained colorless (3 × 15 mL) and the solid obtained was dried in vacuo and stored under nitrogen.

$[MoO_2\{(C_6H_5CO)_2CH\}_2]$ (3): The desired product was obtained as a bright-yellow solid (63 %, 2.72 g, 4.74 mmol). Single crystals suitable for X-ray crystallography were obtained by slow vapor diffusion of diethyl ether into a dichloromethane solution at room temperature. ^1H NMR ($[D_8]$thf): δ = 7.34–7.38 (m, 6 H, CH, *m*-Ar′H), 7.46–7.60 (m, 8 H, *m*-ArH, *p*-ArH, *p*-Ar′H), 8.02 (d, ^3J = 7.6 Hz, 4 H, *o*-Ar′H), 8.16 (d, ^3J = 7.7 Hz, 4 H, *o*-ArH) ppm. The assignments were confirmed by COSY NMR spectroscopy. ^{13}C NMR ($[D_8]$thf): δ = 97.7 [C(O)*C*H], 128.7 (*o*-ArC), 129.0 (*o*-Ar′C), 129.2 (*m*-Ar′C), 129.3 (*m*-ArC), 133.1 (*p*-Ar′C), 133.8 (*p*-ArC), 137.2 (*ipso*-Ar′C), 137.7 (*ipso*-ArC), 180.6 (C′O), 188.4 (CO) ppm. IR: $\tilde{\nu}$ = 3061 (w), 1594 (m), 1544 (s), 1506 (vs), 1474 (vs), 1437 (s), 1354 (m), 1313 (s), 1290 (vs), 1228 (s), 1063 (m), 929 (m), 898 (vs), 755 (m), 708 (m), 676 (m) cm^{-1}. UV/Vis (thf): λ (ε) = 376 (2.97×10^4), 346 nm (2.01×10^4 $L\,mol^{-1}\,cm^{-1}$). MS (ESI): calcd. for $[M - O]^+$ 560.0529; found 560.0577; calcd. for $[M + H]^+$ 577.0556; found 577.0548; calcd. for $[M + Na]^+$ 599.0375; found 599.0496; calcd. for $[M + MeCN + Na]^+$ 640.0641; found 640.0761.

$[MoO_2(C_6H_5COCHCOCH_3)_2]$ (4): The general synthetic procedure was followed using 1-benzoylacetone (2.58 g, 5.9 mmol) as the ligand. The desired product was obtained as a light-green solid (81 %, 2.90 g, 6.42 mmol) as three different conformational isomers. Single crystals suitable for X-ray crystallography were obtained by slow evaporation of a dichloromethane solution at room temperature. ^1H NMR ($[D_8]$thf): δ = 2.17, 2.24, 2.26, 2.29 (s, total 6 H, CH_3), 6.57, 6.63, 6.66, 6.67 (s, total 2 H, CH), 7.44 (t, ^3J = 7.7 Hz, 2 H, *m*-ArH), 7.46–7.53 (m, 4 H, *m*-ArH, *p*-ArH), 7.89 (t, ^3J = 7.6 Hz, 2 H, *o*-ArH), 7.98 (t, ^3J = 6.6 Hz, 2 H, *o*-ArH) ppm. The assignments were confirmed by COSY NMR spectroscopy. ^{13}C NMR ($[D_8]$thf): δ = 25.7, 26.0, 27.1, 28.2 (CH_3), 99.7, 100.7, 101.2, 101.3 (CH), 127.6–129.3 (*o*-ArC, *m*-ArC overlapping), 132.9, 133.1, 133.7, 133.8 (*p*-ArC), 136.4, 136.6, 137.1, 137.2 (*ipso*-ArC), 178.0, 187.0, 187.1, 187.2 187.9, 188.0, 188.1, 198.0 (Ar-CO, $COCH_3$) ppm. IR: $\tilde{\nu}$ = 1592 (m), 1574 (m), 1497 (vs), 1480 (vs), 1450 (s), 1357 (vs), 1283 (vs), 1103 (m), 927 (vs), 899 (vs), 778 (m), 767 (s), 700 (vs), 683 (vs) cm^{-1}. UV/Vis (thf): λ (ε) = 346.0 (4.73×10^4 $L\,mol^{-1}\,cm^{-1}$). MS (ESI): calcd. for $[M - O]^+$ 436.0213; found 436.02332.

$[MoO_2\{(CH_3OC_6H_5CO)_2CH\}_2]$ (5): The general synthetic procedure was followed using bis(*p*-methoxybenzoyl)methane (0.48 g, 1.69 mmol) as the ligand. The desired product was obtained as an orange solid (52 %, 0.31 g, 0.44 mmol). ^1H NMR ($[D_8]$thf): δ = 3.77, 3.88 (s, 12 H, OCH_3), 6.85 (d, ^3J = 9.2 Hz, 4 H, *m*-ArH), 7.03 (d, ^3J = 8.8 Hz, 4 H, *m*-Ar′H), 7.19 (s, 2 H, CH), 7.96 (d, ^3J = 8.8 Hz, 4 H, *o*-ArH), 8.12 (d, ^3J = 8.8 Hz, 4 H, *o*-Ar′H) ppm. The assignments were confirmed by COSY NMR spectroscopy. IR: $\tilde{\nu}$ = 1600 (m), 1544 (m), 1480 (vs), 1456 (vs), 1439 (s), 1300 (m), 1258 (vs), 1227 (vs), 1169 (vs), 1126 (m), 1021 (m), 926 (m), 899 (m), 842 (m), 787 (vs) cm^{-1}. UV/Vis (thf): λ (ε) = 380 (4.08×10^4), 363 (4.73×10^4 $L\,mol^{-1}\,cm^{-1}$). MS (ESI): calcd. for $[M + H]^+$ 697.0980; found 697.989; calcd. for $[M - O]^+$ 680.0953; found 680.0941.

$[MoO_2\{(C_5H_6O)COCH_3\}_2]$ (6): The general synthetic procedure was followed using 2-acetylcyclopentanone (0.41 g, 3.25 mmol) as the ligand. The desired product was obtained as a dark-green solid (53 %, 0.28 g, 0.74 mmol). ^1H NMR ($[D_8]$thf): δ = 1.85–1.97 (m, 4 H, $CH_2CH_2CH_2$), 2.05, 2.06, 2.09, 2.09 (s, 6 H, CH_3), 2.29–2.56 (m, 4 H, CCH_2), 2.63–2.72 (m, 4 H, $COCH_2$) ppm. The assignments were confirmed by COSY NMR spectroscopy. IR: $\tilde{\nu}$ = 3299 (w), 1595 (m), 1489 (vs), 1272 (m), 1241 (s), 935 (s), 901 (vs), 831 (m), 791 (m), 727 (m) cm^{-1}. UV/Vis (thf): λ (ε) = 332 (4.38×10^5), 777 (264 $L\,mol^{-1}\,cm^{-1}$). MS (ESI): calcd. for $[M + CH_3CN + Na]^+$ 444.0324; found 444.0285.

$[MoO_2\{(C_6H_8O)COCH_3\}_2]$ (7): The general synthetic procedure was followed using 2-acetylcyclohexanone (1.02 g, 7.28 mmol) as the ligand, with the exception that the ethanol was removed in vacuo before cooling overnight. The desired product was obtained as a dark-blue solid (44 %, 0.66 g, 1.61 mmol). ^1H NMR ($[D_8]$thf): δ = 1.62–1.68 (m, 8 H, $CH_2CH_2CH_2CH_2$, $CH_2CH_2CH_2CH_2$), 2.06, 2.06, 2.13, 2.15 (s, 6 H, CH_3), 2.23–2.46 (m, 8 H, $COCH_2$, CCH_2) ppm. The assignments were confirmed by COSY NMR spectroscopy. IR: $\tilde{\nu}$ = 3351 (br w), 2959 (w), 2878 (w), 1563 (s), 1474 (s), 1290 (vs), 940 (s), 893 (vs), 800 (m), 772 (s) cm^{-1}. UV/Vis (thf): λ (ε) = 289 (1.65×10^3), 778 (329 $L\,mol^{-1}\,cm^{-1}$). MS (ESI): calcd. for $[M + CH_3CN + Na]^+$ 472.0638; found 472.0552; calcd. for $[M + Na]^+$ 431.0372; found 431.0361.

[$MoO_2\{(C_{12}H_8O)COCH_3\}_2$] (8): The general synthetic procedure was followed using 2-acetyl-1-tetralone (2.48 g, 13.2 mmol) as the ligand. The desired product was obtained as a yellow solid (80%, 2.65 g, 5.28 mmol). Single crystals suitable for X-ray crystallography were obtained by slow evaporation of a dichloromethane solution at 2 °C. ^1H NMR ([D$_8$]thf): δ = 2.28 (s, 6 H, CH_3), 2.77 (m, 4 H, Ar-CH_2), 2.89 (m, 4 H, CCH_2), 7.23 (d, ^3J = 7.6 Hz, 2 H, 5-ArH), 7.31 (t, ^3J = 8.0 Hz, 2 H, 3-ArH), 7.38 (t, ^3J = 7.2 Hz, 2 H, 4-ArH), 7.97 (d, ^3J = 7.2 Hz, 2 H, 2-ArH) ppm. The assignments were confirmed by COSY NMR spectroscopy. IR: $\tilde{\nu}$ = 2941 (w), 2890 (w), 2838 (w), 1587 (m), 1562 (m), 1464 (vs), 1448 (vs), 1357 (s), 1295 (s), 927 (s), 897 (vs), 737 (s), 720 (m) cm^{-1}. UV/Vis (thf): λ (ε) = 376 (1.47×10^4 L mol^{-1} cm^{-1}). MS (ESI): calcd. for [M + CH_3CN + Na]$^+$ 568.0640; found 568.0566; calcd. for [M + Na]$^+$ 527.0374; found 527.0419; calcd. for [M – O]$^+$ 488.0527; found 488.0450.

X-ray Crystallography: Single crystals of suitable dimension were used for data collection. Reflections were measured with a Nonius–KappaCCD diffractometer (compounds **3** and **4**) with rotating anode and graphite monochromator (λ = 0.71073 Å) or with a Bruker Kappa ApexII diffractometer (compound **8**) with sealed tube and Triumph monochromator (λ = 0.71073 Å) up to a resolution of $(\sin\theta/\lambda_{max})$ = 0.65 Å^{-1} at a temperature of 110(2) (**3**) or 150(2) K (**4** and **8**). The reflections were integrated with EVAL14[34] (**3**), EVAL15[35] (**4**), or SAINT[36] (**8**) software. Absorption corrections based on multiple measured reflections were performed with SADABS.[37] The structures were solved by direct methods using SHELXS-97[38] and refined with SHELXL-97 against F^2 for all reflections. Non-hydrogen atoms were refined freely with anisotropic displacement parameters. All hydrogen atoms were located in difference Fourier maps (**3** and **4**) or introduced at calculated positions (**8**) and refined with a riding model. The structure of **8** was refined as an inversion twin[27] resulting in a twin fraction of 0.15(2). Geometry calculations and checking for higher symmetry was performed with the PLATON program.[39]

CCDC-910320 (for **3**), -910321 (for **4**), and -910322 (for **8**) contain the supplementary crystallographic data for this paper. These data can be obtained free of charge from The Cambridge Crystallographic Data Centre via www.ccdc.cam.ac.uk/data_request/cif.

Typical Procedure for the Dehydration of Alcohols to Olefins: A solution of substrate (2 mmol) and pentadecane as internal standard (250 µL, 192.3 mg) in toluene (10 mL) was added to the catalyst. The reaction flask was sealed with a septum, placed in a preheated aluminum block-heater at 100 °C, and stirred magnetically. Samples for GC analysis were removed by syringe, filtered through Florisil, and eluted with ethyl acetate. For the reactions analyzed by NMR, [D$_8$]toluene was used as the solvent and the yield was determined against 1,3,5-trimethoxybenzene (0.67 mmol, 112.1 mg) as internal standard. When using a liquid catalyst, the same procedure was used, but the catalyst was added to the solution by Finnpipette. For the reactions at 150 °C, the same procedure was used but in a 50 mL Parr autoclave using a glass insert and mechanical stirring.

Supporting Information (see footnote on the first page of this article): ^1H, ^{13}C, and COSY NMR, IR, UV/Vis, and ESI-MS spectra for complexes **1**–**8**.

Acknowledgments

This research was performed within the framework of the CatchBio program. The authors gratefully acknowledge the support of the Smart Mix Program of the Netherlands Ministry of Economic Affairs, Agriculture and Innovation and the Netherlands Ministry of Education, Culture and Science.

---

[1] R. D. Perlack, L. L. Wright, A. F. Turhollow, R. L. Graham, B. J. Stokes, D. C. Erbach, *Biomass as Feedstock for a Bioenergy and Bioproducts Industry: The Technical Feasibility of a Billion-Ton Annual Supply*, U.S. Department of Energy and U.S. Department of Agriculture, Oak Ridge, TN, **2005**.

[2] T. Werpy, G. Peterson, *Top Value Added Chemicals from Biomass*, vol. 1, *Results of Screening for Potential Candidates from Sugars and Synthesis Gas*, U.S. Department of Energy, Oak Ridge, TN, **2004**.

[3] M.-H. Lee, S.-W. Lee, Y.-M. Jeon, D.-Y. Park, J.-Y. Ryu, *Novel method for preparing styrenic olefins*, LG Chemical Ltd., World Patent 2005/035468, **2005**.

[4] W. R. Moser, R. W. Thompson, C.-C. Chiang, H. Tong, *J. Catal.* **1989**, *117*, 19–32.

[5] H. Dirkzwager, M. van Zwienen, *Process for the preparation of styrenes*, Shell International Research, World Patent 99/58480, **1999**.

[6] G. Larsen, E. Lotero, L. M. Petkovic, D. S. Shobe, *J. Catal.* **1997**, *169*, 67–75.

[7] M. H. Lee, E. T. Choi, D. Kim, Y. M. Lee, Y. S. Park, *Eur. J. Org. Chem.* **2008**, 5630–5637.

[8] M. Schlaf, P. Ghosh, P. J. Fagan, E. Hauptman, R. M. Bullock, *Angew. Chem.* **2001**, *113*, 4005; *Angew. Chem. Int. Ed.* **2001**, *40*, 3887–3890.

[9] Z. Zhu, J. H. Espenson, *J. Org. Chem.* **1996**, *61*, 324–328.

[10] J. Ziegler, M. Zdilla, A. Evans, M. M. Abu-Omar, *Inorg. Chem.* **2009**, *48*, 9998–10000.

[11] E. Arceo, J. Ellman, R. Bergman, *J. Am. Chem. Soc.* **2010**, *132*, 11408–11409.

[12] S. Vkuturi, G. Chapman, I. Ahmad, K. M. Nicholas, *Inorg. Chem.* **2010**, *49*, 4744–4746.

[13] I. Ahmad, G. Chapman, K. M. Nicholas, *Organometallics* **2011**, *30*, 2810–2818.

[14] T. J. Korstanje, J. T. B. H. Jastrzebski, R. J. M. Klein Gebbink, *ChemSusChem* **2010**, *3*, 695–697.

[15] T. J. Korstanje, E. F. de Waard, J. T. B. H. Jastrzebski, R. J. M. Klein Gebbink, *ACS Catal.* **2012**, *2*, 2173–2181.

[16] M. L. Kantam, A. D. Prasad, P. L. Santhi, *Synth. Commun.* **1993**, *23*, 45–48.

[17] C. Kisker, H. Schindelin, D. Rees, *Annu. Rev. Biochem.* **1997**, *66*, 233–267.

[18] H. Vrubel, V. Verzenhassi, S. Nakagaki, F. Nunes, *Inorg. Chem. Commun.* **2008**, *11*, 1040–1043.

[19] F. Moore, R. Rice, *Inorg. Chem.* **1968**, *7*, 2510–2514.

[20] W. Griffith, T. Wickins, *J. Chem. Soc. A* **1968**, 400–404.

[21] A. A. Bugayev, S. E. Nikitin, *Opt. Commun.* **2000**, *180*, 69–71.

[22] M. Brown, B. Cook, T. Sloan, *Inorg. Chem.* **1975**, *14*, 1273–1278.

[23] B. Kamenar, M. Penavic, C. K. Prout, *Cryst. Struct. Commun.* **1973**, *2*, 41–44.

[24] O. Krasochka, Y. Sokolova, L. Atovmyan, *J. Struct. Chem.* **1975**, *16*, 648–650.

[25] M. Nass, M. Schurmann, H. Preut, N. Krause, *Z. Kristallogr. New Cryst. Struct.* **2001**, *216*, 461–464.

[26] B. Kojic-Prodic, Z. Rudic-Toros, D. Grdenic, L. Golic, *Acta Crystallogr., Sect. B* **1974**, *30*, 300–305.

[27] H. Flack, *Acta Crystallogr., Sect. A* **1983**, *39*, 876–881.

[28] A. Vasishtha, R. Trivedi, G. Das, *J. Am. Oil Chem. Soc.* **1990**, *67*, 333–337.

[29] P. van Leeuwen, N. Clement, M. Tschan, *Coord. Chem. Rev.* **2011**, *255*, 1499–1517.

[30] H. Gehrke Jr., J. Veal, *Inorg. Chim. Acta* **1969**, *3*, 623–627.

[31] I. Bernal, *Chem. Ind.* **1966**, 1343–1344.

[32] M. Peterson, R. Vanatta, R. Richman, *Inorg. Chem.* **1983**, *22*, 1982–1985.

[33] W. Franek, *Monatsh. Chem.* **1996**, *127*, 895–907.

[34] A. J. M. Duisenberg, L. M. J. Kroon-Batenburg, A. M. M. Schreurs, *J. Appl. Crystallogr.* **2003**, *36*, 220–229.
[35] A. M. M. Schreurs, X. Y. Xian, L. M. J. Kroon-Batenburg, *J. Appl. Crystallogr.* **2010**, *43*, 70–82.
[36] *SAINT-Plus*, Bruxer AXS Inc., Madison, WI, **2001**.
[37] G. M. Sheldrick, *SADABS: Area-Detector Absorption Correction*, v. 2.10, University of Göttingen, Germany, **1999**.
[38] G. M. Sheldrick, *Acta Crystallogr., Sect. A* **2008**, *64*, 112–122.
[39] A. L. Spek, *Acta Crystallogr., Sect. D* **2009**, *65*, 148–155.

Received: November 8, 2012